Aalborg Universitet

Drained True Triaxial Tests on Aalborg University Sand No 0

Praastrup, U.

Publication date:
2000

Document Version
Publisher's PDF, also known as Version of record

Link to publication from Aalborg University

Citation for published version (APA):
Praastrup, U. (2000). *Drained True Triaxial Tests on Aalborg University Sand No 0*. Geotechnical Engineering Group. AAU Geotechnical Engineering Papers : Laboratory Testing Paper Vol. R2009 No. 34

General rights
Copyright and moral rights for the publications made accessible in the public portal are retained by the authors and/or other copyright owners and it is a condition of accessing publications that users recognise and abide by the legal requirements associated with these rights.

- Users may download and print one copy of any publication from the public portal for the purpose of private study or research.
- You may not further distribute the material or use it for any profit-making activity or commercial gain
- You may freely distribute the URL identifying the publication in the public portal -

Take down policy
If you believe that this document breaches copyright please contact us at vbn@aub.aau.dk providing details, and we will remove access to the work immediately and investigate your claim.

Downloaded from vbn.aau.dk on: December 15, 2025

AAU Geotechnical Engineering Papers ISSN 1398-6465 R 2009

Drained True Triaxal Tests on Aalborg University Sand No 0

U. Praastrup

2000 Laboratory testing paper no 34

GEOTECHNICAL ENGINEERING GROUP
AALBORG UNIVERSITY DENMARK

Drained True Triaxial Tests on Aalborg University Sand No 0

Ulrik Praastrup
Aalborg University, Aalborg, Denmark

Abstract: The paper presents the first series of true triaxial tests carried out on air-pluviated unfrozen and frozen specimens of Aalborg University Sand No 0. The specimens have been tested in the newly improved version of the Danish rigid boundary true triaxial apparatus to optimise the preparation and installation techniques for testing sand in the apparatus. The tests have also formed the basis for implementing, testing and modifying a quite complex data collection and control software package. Moreover, some of tests were designed to investigate the anisotropy of the specimens. The optimised techniques used for preparing the unfrozen and frozen sand specimens are together with the installation of the specimens into the apparatus outlined in terms of a photo gallery. Furthermore, the gallery includes photos showing how to install frozen specimens into a conventional triaxial apparatus.

Conclusion: The findings of this work can be summarised as follows. True triaxial tests on unfrozen sand specimens cannot be recommended to form the basis for future research using the techniques outlined in this paper. The unfrozen specimens cannot be shaped in a satisfactory manner using the split mould and the membranes made to prepare these specimens. The scatter in the test results is found to be high when compared with similar test results found in the literature. However, the tests can be used for comparison purposes and perhaps guide one in a certain direction. Nevertheless, tests on both unfrozen and frozen specimens reveal that the specimens behave in a cross-anisotropic manner, e.g. the strength depends on the direction in which they are sheared. More reliable test results have been obtained from tests on frozen sand specimens and the techniques for preparing these specimens have been developed with success. It is found that tests on frozen specimens should form the basis for future research.

1 INTRODUCTION

The true triaxial tests have been carried out in the newly improved version of the Danish rigid boundary true triaxial apparatus, which is located at Aalborg University. The innermost part of the apparatus consists of a system of nested rigid platens that was brilliantly developed by Hambly in 1967.

The first rigid boundary true triaxial apparatus was built at Cambridge University by Pearce (1972), who also reported the first test results. The Danish version of this apparatus was originally built by M. Jacobsen in the late seventies but it has since been significantly improved by L.B. Ibsen and the author of this paper.

A detailed description of the apparatus can be found in Ibsen & Praastrup (2000). For the record, it should be mentioned that only a few rigid boundary apparatuses exist in the world. This is most likely because of the great expense involved in building such an apparatus and the expertise needed to carry out the tests. Besides the present equipment the author is aware of an apparatus in Germany, which was build by Gudehus (1971).

1.1 Instrumentation and software

The data collection from the apparatus has been fully automated using "state-of-the-art" instrumentation and a package of custom-made software. The software package is together with some electronic devises capable of controlling the movement of the rigid platens and this control can be done in terms of principal stresses, principal strains or a combination of these. It is, of course, not possible to control both the stress and the strain in the same direction and at the same time. However, one direction can be stress controlled while the others are strain controlled and vice versa. It is for example possible to carry out an oedometer test (on a cubical specimen) in which the strains are held constant in two directions together with a constant total stress in the third direction.

The instrumentation of the apparatus is described in Ibsen & Praastrup (2000) and can be summarised as follows. The three principal stresses are measured by three load cells. One load cell is placed in each of the three directions determined by the apparatus. The three displacements (principal strains) are measured by six inductive displacement transducers, which have been coupled two by two to prevent the measurement of rigid body motions. The three load cells and the six displacement transducers are all connected to a MGC+ amplifier device, from where the movement of the platens is controlled by use of the mentioned software package. The pore pressure is measured by an absolute pressure transducer, which is connected to a MVD2555 amplifier device. The volume change is measured by a scale but may also be measured by a back pressure system.

The amplifier devices (including the scale) are all connected to a personal computer, where the software package is installed under Windows 3.1. The software package consists of a main program (called *cubmenul.txt*) and supplementary programs, which are used to configure the electronic system. The supplementary programs are similar to the programs made to carry out tests in a conventional triaxial apparatus (Praastrup, 1999a,b & 2000c).

The main program controls a test in terms of total principal stresses or principal strains in virtually any desired manner and collects all necessary data while running a test. The program is similar to the program developed for conventional triaxial testing (Praastrup, 1999b & 2000c) except for the fact that a third principal stress and principal strain component has been built into the present program.

More details on the programs can be found in the comments typed into the programs. The programs can be found on an institute server (//indy/geotek) for some time after the publication of this paper and on the CD-ROM published with the author's Ph.D.-dissertation.

2 TEST PROCEDURES

This section will in general terms explain how the tests have been carried out and discuss some of the test results.

2.1 Sand tested

The tests have all been carried out on dense specimens of Aalborg University Sand No 0, with void ratios of 0.61±0.004.

The sand has been extensively tested in the laboratory and details can be found in e.g. Ibsen & Bødker (1994), Borup & Hedegaard (1995) and Ibsen & Praastrup (2000). The classification properties for the sand are summarised in table 1.

Table 1. Classification properties for Aalborg University Sand No 0.

Parameter	Value
Mean diameter [mm]	0.14
Coefficient of uniformity	1.78
Maximum grain size [mm]	1.00
Specific gravity of grains	2.64
Maximum void ratio	0.85
Minimum void ratio	0.55

2.2 Preparation

The specimens have all been deposited by air-pluviation, which is the standard method used for preparing sand specimens. The first series of tests was carried out on unfrozen specimens, whereas the other and final series were carried out on (mainly) frozen specimens. Details are found in the photo gallery and in Ibsen & Praastrup (2000).

2.3 Saturation

The specimens have all been saturated with deaired and deionized water. The specimens were first flushed through with carbon dioxide before deaired and deionized water was introduced to the specimens. A detailed description of the saturation process can be found in Jakobsen (1998) and in Jakobsen & Praastrup (1998). Details can also be found in the photo gallery, the program *cubmenul.txt* and on the data files placed on the CD-ROM. Maximum saturation pressure for each test has been included in the enclosed data sheets.

2.3.1 Consolidation

After saturation, most specimens were isotropically consolidated to a predetermined hydrostatic pressure. The consolidation process was in average carried out at no more than 5 kPa/min. The exact data can be found on the CD-ROM, whereas minimum and maximum pressures can be found in the enclosed data sheets.

2.3.2 Shearing

The specimens were all sheared right after consolidation (or right after saturation for tests that were not consolidated prior to shear). The tests can be grouped into two categories. The first category includes the tests that were carried out as conventional triaxial compression tests, where the minor and intermediate stresses are held constant during shear. Most of the tests were performed to optimise the preparation and installation techniques. Tests on frozen and unfrozen specimens have been carried out at different constant confining pressures of 40, 80, 160, 320 and 640 kPa. Tests on unfrozen specimens revealed that testing above 320 kPa at constant confining pressure should be avoided. For tests carried out above this pressure the gaps between the rigid platens became so large that the membrane could slip out through the gaps. The most successful tests were carried out in the range from 40 to 160 kPa.

The purpose of the tests carried out on the frozen specimens (with constant confining pressures) was twofold. Firstly, the tests were carried out to examine the effects on the test results of some smaller variations in the saturation technique. The test results show that the best test results were obtained when the technique described in Ibsen & Praastrup (2000) was used. Secondly, the tests were carried out to investigate the effect of using lubricated interfaces between the specimen and the rigid platens. The test results show that consistent results can be obtained when testing frozen specimens using lubricated platens. For tests on specimens coated with just a single layer of grease inconsistencies were observed in the measured secant friction angles and on the stress-strain curves. Furthermore, it was found that the sensor heads should be placed parallel to the surface of the platens or slightly above to produce consistent test results (see figure 40). Inconsistencies in the secant friction angle and in the stress-strain curves were observed in tests where the sensor heads were positioned below the surfaces of the platens.

The tests in the second category have all been carried out as constant mean effective stress tests. Based on the above findings the tests were carried out at a mean effective stress of 160 kPa. Moreover, the specimens were sheared with a constant value of b (e.g. Ibsen & Praastrup, 2000). The constant mean effective stress tests performed on the unfrozen specimens showed that it was not possible to shear specimens with a strain rate lower than approximately 8%/h. The average strain rate was approximately 12%/h in these tests and the specimens could, furthermore, not be sheared at a constant strain rate. This is found inadequate within static geotechnical testing.

The apparatus was, therefore, rebuilt and a set of new motors was installed to replace the older one. Moreover, a new gear system was built into the apparatus with DC-tacho control on the new motors. The lower limit on the strain rate is now 1.0%/h and the motors can quite accurately produce a constant strain rate. Succeeding tests were sheared at a constant strain rate of approximately 2%/h. The test results show that the stress-strain and strenght behaviour of the specimens is cross-anisotropic. This is illustrated figure 1, where the secant friction angles for tests on unfrozen specimens have been plotted against *b*. More details can be found in Ibsen & Praastrup (2000) and in the enclosed data sheets.

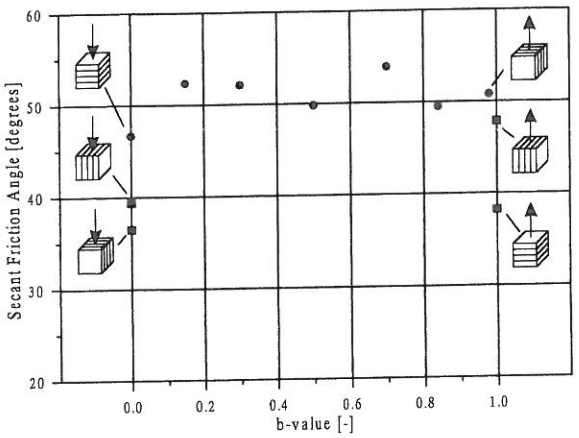

Fig. 1. Secant friction angles for true triaxial tests on unfrozen specimens plotted against b.

3 PRESENTATION OF TEST RESULTS

The test results shown on the enclosed data sheets are presented in a very straight forward manner to simplify the interpretation of the tests. There is one data sheet for each test and only four diagrams on each sheet. The diagrams are explained in what follows. The diagram on the top left shows the deviator stress plotted against the measured displacements. The deviator stress is determined as the major principal stress minus the minor principal stress. The precise calculations of the stresses and the displacements are given in succeeding subsections. The diagram on the top right shows two volume change curves plotted against the largest displacement. One curve is based on the weight measurements, whereas the other curve is based on the displacement measurements. The first mentioned curve is located above the other curve or in rare cases right on this curve as seen from the data sheets. The gap between the two curves is primarily caused by compression of the lubrication system on the rigid platens and the fact that the specimen has to adjust its shape to the cavity determined by the rigid platens. The calculation of the two volume changes is outlined in succeeding subsections. The diagram on the bottom left shows the measured displacements plotted against the volume change measured by the scale. The above mentioned diagrams have all been plotted by means of data collected during shear. The last diagram (positioned on the bottom right) shows data collected during isotropic consolidation. The diagram includes four curves plotted against the volume change measured by the scale. Three of the curves show the measured displacements, whereas the fourth and final curve shows the displacement calculated from the volume change. The fourth curve (termed iso.) has been obtained under the assumptions that the specimens behave isotropically and that the strains are small (e.g. Praastrup et al., 1999). The relations (1), (2) and (3) have been used to obtain the fourth curve:

$$\varepsilon_v(t) = \varepsilon_1(t) + \varepsilon_2(t) + \varepsilon_3(t) \tag{1}$$

$$\varepsilon_v(t) = \frac{\Delta V(t)}{V}; \varepsilon_i(t) = \frac{u_i(t)}{L} \tag{2}$$

$$u_i(t) = \frac{L}{3}\varepsilon_v(t) \tag{3}$$

where;

- ε_v: Volumetric strain [%].
- ε_i: Linear strain in direction i [%].
- ΔV: Volume change [cm^3].
- u_i: Displacement in direction i [mm].
- L: Initial height, length and width of specimen [mm].
- V: Initial volume of specimen [cm^3].
- t: time.
- t_o: time of reference.
- i: direction 1, 2 or 3.

As seen from the data sheets, the relative positions of the curves indicate that the displacements measured during isotropic consolidation cannot be trusted. The measured displacements are simply too small compared with the errors on the displacements caused by e.g. the compression of lubrication system on the rigid platens.

The only reliable deformation measurement comes from the weight. The displacements measured during saturation cannot be trusted either. For more compressible specimens the above conclusion might be incorrect because it depends on the magnitude of the displacements. For the tests presented in this paper the magnitude of the displacements (during consolidation) is in the order of 0.1-0.3 mm.

3.1 Calculations

The following subsections deal with the calculations of the deformations and the loads.

3.1.1 Stresses

The principal stresses are calculated directly from load cell measurements using the following relation:

$$\sigma_i(t) = (LC_i(t) - LC_i(t_0))a_i \quad (4)$$

where;

σ_i: Cauchy stress in direction i [kPa].
LC_i: Load cell measurement in direction i [kg].
a_i: Calibration factor for direction i [kPa/kg].

The reference points for the stresses are taken prior to the installation of the specimen into the apparatus.

The three calibration factors are determined by applying different hydrostatic pressures to an empty membrane placed inside the apparatus.

3.1.2 Displacements

The displacements are calculated directly from two opposite positioned displacement transducers as follows:

$$u_i(t) = (DT_i(t) - DT_i(t_0))\beta_i \quad (5)$$

where;

DT_i: Displacement transducer measurement in direction i [V].
β_i: Calibration factor in direction i [mm/V].

The reference points for the displacements are taken right after saturation, e.i. they are not taken at the same time as the reference point for the stresses. The calibration factors are determined using a sensitive calibration bench.

3.1.3 Volume change

As mentioned previously, the volume change can be calculated in two different ways. Compression is of course considered positive. The volume change can be calculated from the weight measurements as follows:

$$\Delta V(t) = (W(t) - W(t_0))\gamma \quad (6)$$

where;

W: Weight measurement [g].
γ: Calibration factor [cm^3/g].

The reference point for the scale is taken right after saturation, i.e. it is taken at the same time as the reference points for the displacements. The volume change can also be determined from the displacement measurement:

$$\Delta V(t) = V - (L - u_1(t))(L - u_2(t))(L - u_3(t)) \quad (7)$$

As mentioned previously and in Ibsen & Praastrup (2000) the relations in (6) and (7) should produce the same value for the volume change but this is as mentioned not the case. Ibsen & Praastrup (2000) have suggested a suitable correction scheme to obtain a consistent displacement field. The displacements shown on the enclosed data sheets have not been corrected using this correction scheme or any other correction scheme at all. Some examples on how to apply the correction scheme can be found on the CD-ROM.

3.1.4 Pore pressure

The absolute pore pressure is measured directly. The pore pressure is set to zero right

after saturation. The pore pressure has been measured in almost every test and fluctuations from the zero level are typically below 1 kPa. Values for the pore pressures have not been included in the enclosed data sheets but they can be found on the CD-ROM.

4 PHOTO GALLERY

This section shows some photos taken to illustrate the optimised experimental procedures that have been developed during the author's work on the apparatus. The section is divided into three subsections; specimen preparation, installation and miscellaneous. The first subsection includes photos of how to prepare air-pluviated frozen and unfrozen specimens prior to their installation into the apparatus. It should be mentioned that several adjustments of the procedures have been tested and that the photo gallery only deals with the optimised procedures. The second subsection shows how the frozen specimens are installed into the true and into the conventional triaxial apparatus. The third subsection includes miscellaneous photos, which have been taken to illustrate certain issues. The photos can also be found on the CD-ROM. Finally, it should be mentioned that most of the equipment shown in the photos has been produced by the skilful laboratory technician J. C. Ildahl.

4.1 Specimen preparation

The frozen and unfrozen sand specimens are treated in the above order.

4.1.1 Frozen sand specimens

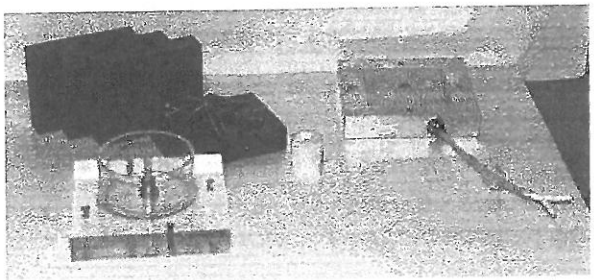

Fig. 2. Dismounted split mould for preparing frozen sand specimens. The platens can be mounted together using the screws shown close to the middle of the photo. (Photo No 11).

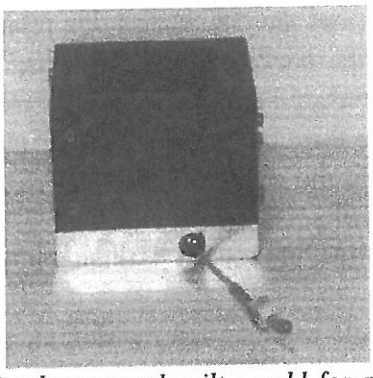

Fig. 3. Partly mounted spilt mould for preparing frozen sand specimen. Top platen not mounted and not shown (Photo No 22).

Fig. 4. Equipment used for preparing air-pluviated sand specimens (frozen and unfrozen). Four large sieves (2x2 mm and 2x1 mm), one small sieve (1 mm), one paper disc, one rubber disc, one plastic funnel and a strainer (Photo No 12).

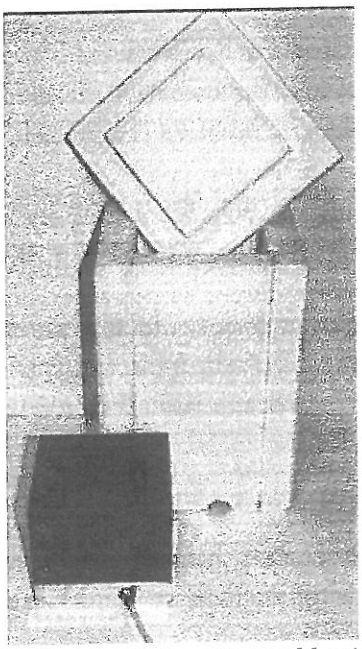

Fig. 5. Partly mounted split mould with a container (referred to as the igloo) made of phoenicopterus rubber (flamingo). (Photo No 23).

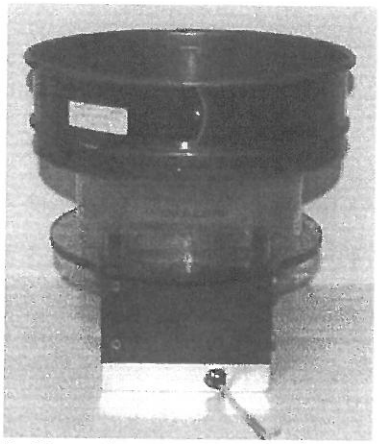

Fig. 6. A hollow plexiglass object placed on top of the partly mounted spilt mould and a large 1 mm sieve placed on top. (Photo No 24).

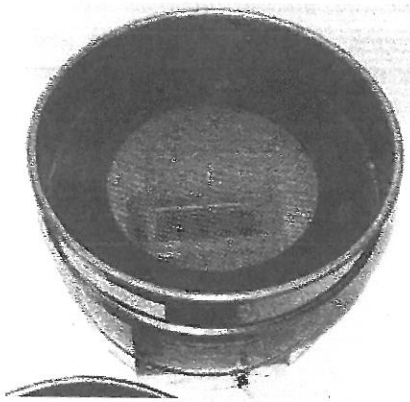

Fig. 7. Rubber disc placed inside the bottom sieve to capture excess grains. The plexiglass object is rectangular on the inside. (Photo No 25).

Fig. 8. Sieves placed on top of the plexiglass object. The two 2 mm sieves are placed in the middle of the two 1 mm sieves. The small sieve is placed on top and its position is determined by the paper disc. The strainer is placed inside the smaller sieve. (Photo No 26).

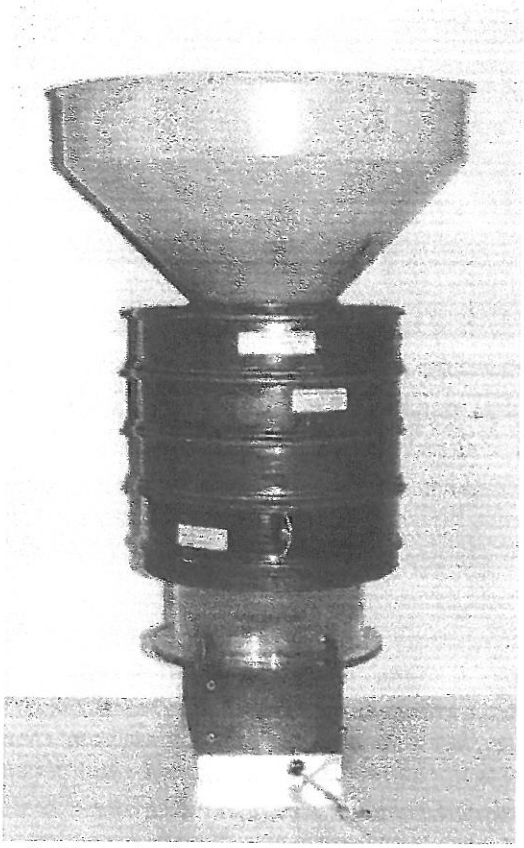

Fig. 9. Funnel placed on top of the sieves. The sand is filled into the funnel after the weight of the sand has been measured. The same amount of sand is used each time. (Photo No 27).

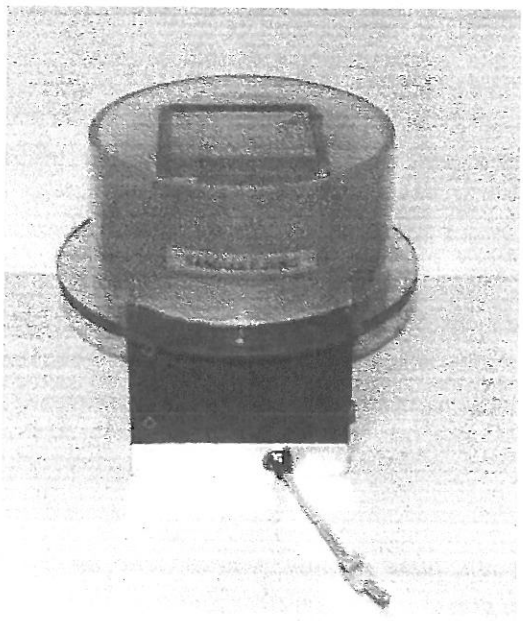

Fig. 10. Partly mounted split mould with the plexiglass object. Sieves, funnel, etc. have been removed and excess grains have been collected for measuring. The preparation procedure is terminated at this stage if the surface of the sand is not horizontal. (Photo No 28).

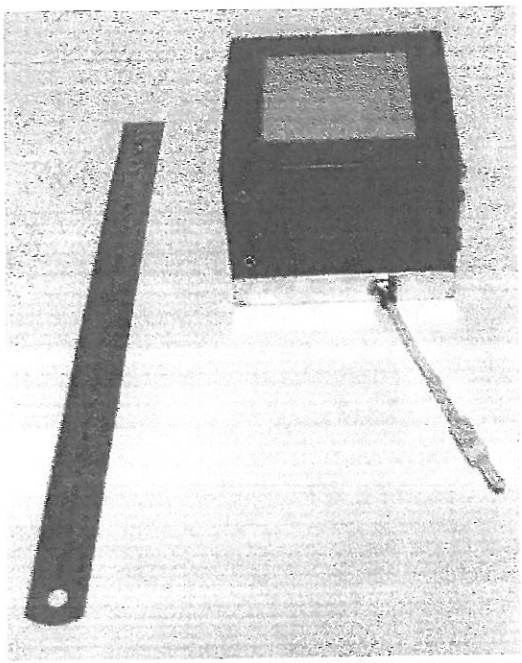

Fig. 11. Sand in partly mounted split mould. Excess grains have been brushed off using the ruler shown in the figure and a vacuum cleaner that is not shown. Finally, the void ratio is calculated and compared with the desired value (0.61 ±0.004). If the value is found acceptable the preparation procedure is continued. (Photo No 29).

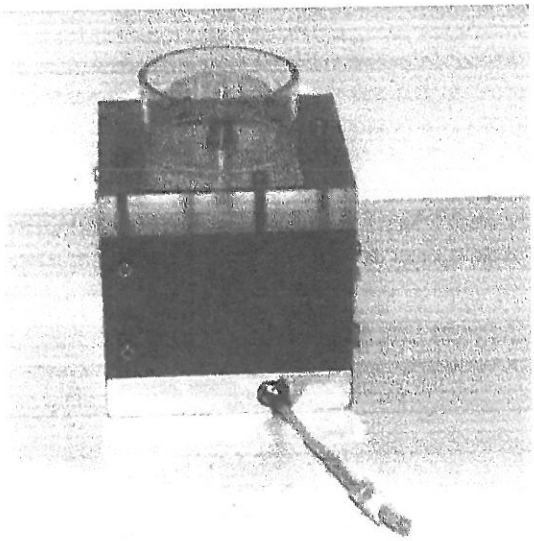

Fig. 12. Sand in fully mounted spilt mould. The spilt mould is now completely watertight since silicone grease has been used on the interfaces of platens. The bottom and top platens have built-in filter stones and drainage lines. The bottom filter stone is connected to the tube sticking out from the bottom plate. The tube can be open or closed. The top filter stone is connected to what is referred to as the "chimney", which is seen in the top of the figure. (Photo No 30).

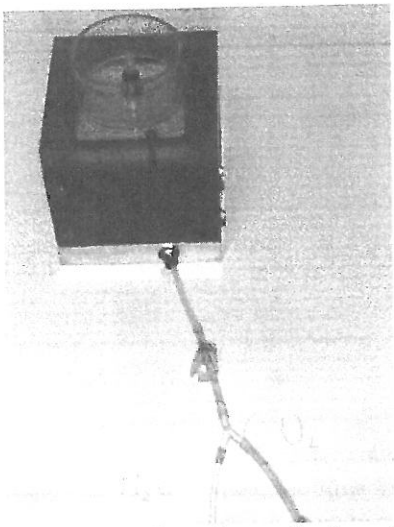

Fig. 13. Saturation of specimen. Carbon dioxide is flushed through the specimen for about 15 min. at approximately 5 kPa. Afterwards deaired and deionized water is introduced to the specimen to obtain the best possible saturation prior to freezing the specimen. (Photo No 31).

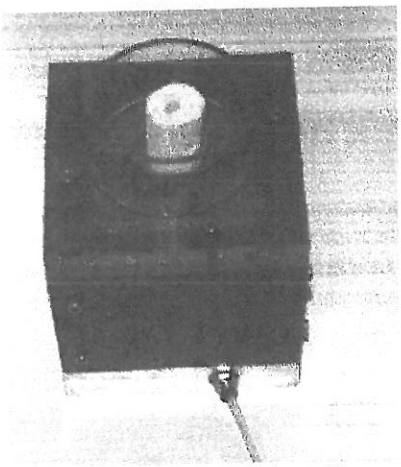

Fig. 14. Water saturated sand in split mould. The white object placed on the chimney is made of flamingo to insulate and therefore delay the freezing of the top of the specimen when put into the freezer. (Photo No 32).

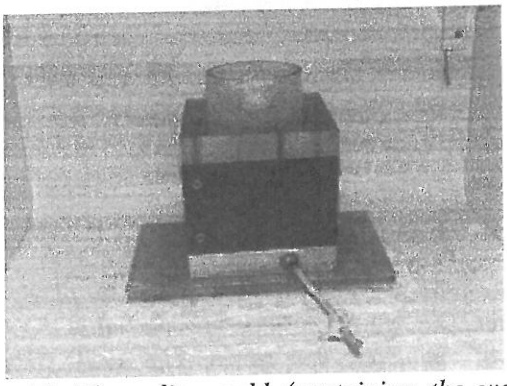

Fig. 15. The split mould (containing the water saturated specimen) placed on a metal plate in the freezer. (Photo No 34).

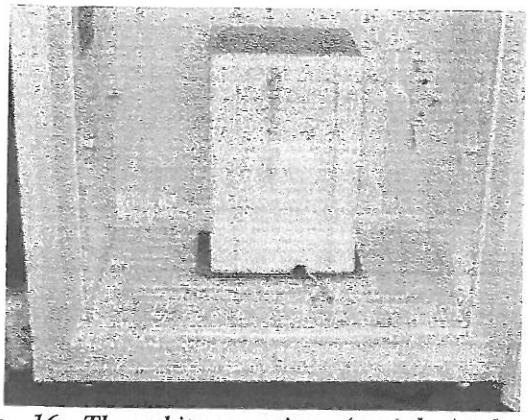

Fig. 16. The white container (or igloo) placed around the split mould. The whole system ensures that the specimen is frozen from the bottom to the top. Excess water is pushed out through the chimney and captured by the container placed on top of the top platen. The tube is of course closed during this phase to hinder the water to slip out. The specimens are typically left in the freezer for approximately eight hours. (Photo No 10).

4.1.2 Unfrozen specimens

The technique for preparing unfrozen sand specimens is quite similar to the technique for preparing frozen specimens. One difference is of course that the freezing of the specimen is omitted in the first procedure. Furthermore, two different split moulds are used. The split mould for preparing unfrozen specimens is shown in the figures 17 and 18.

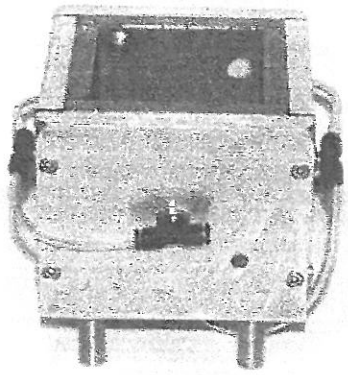

Fig. 17. Fully assembled split mould for preparing unfrozen sand specimens. The tubes are connected with the porous copper seen inside the split mould. The tubes are connected to a vacuum pump, which is used to position the membrane into its rightful position. The holes seen in two of the platens are used to place the drainage gadgets correctly. (Photo No 18).

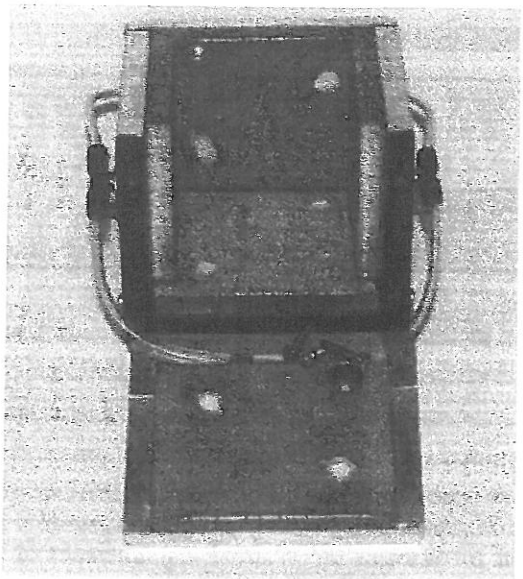

Fig. 18. Partly dismounted split mould for preparing unfrozen sand specimens. The plate located in the back can also be dismounted. The specimens are removed from the spilt mould under a partial vacuum of approximately 20 kPa and subsequently placed in the true triaxial apparatus. (Photo No 19).

As described in Ibsen & Praastrup (2000) the specimens cannot be shaped in a satisfactory manner using this technique and it cannot be recommended to form the basis for future research. The membranes for the unfrozen specimens are larger in one direction (vertical) than the membranes used for the frozen specimens. For the unfrozen specimens the membrane is placed inside the split mould prior to the deposition of the sand, which is not the case for the frozen specimens. The uppermost surface becomes very irregular when the membrane is folded on top of the specimen. Irregularities were also present around the knobs on the membrane. Moreover, it was difficult to obtain sharp corners and to obtain the correct value for the volume of the specimen.

4.2 Installation

This subsection includes photos of how to install frozen specimens into the true triaxial apparatus and into the conventional triaxial apparatus. The installation of the unfrozen specimens is quite similar and photos of this are not shown.

4.2.1 Conventional triaxial apparatus

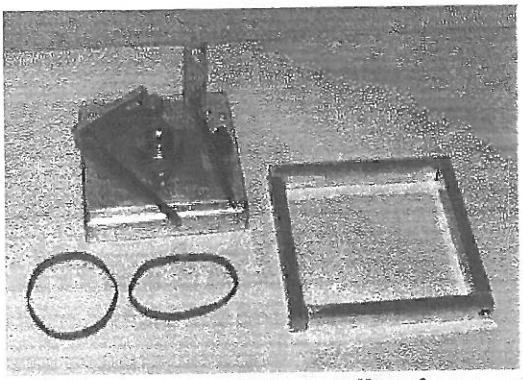

Fig. 19. Equipment used for installing frozen cubical specimens into a conventional triaxial apparatus. The two gadgets placed on the top platen are used to measure the vertical displacement of the specimen during a test. The rubber bands are placed on top of the membrane that surrounds the specimen (not shown). The bars connected in a ring are placed on top of the rubber bands. The system prevents the cell water to connect with the specimen. (Photo No 1).

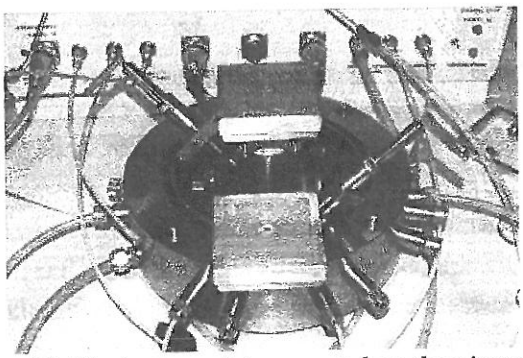

Fig. 20. The bottom plate mounted on the piston in the conventional triaxial apparatus together with the top plate. The platens have both been lubricated using two rubber sheets and two thin layers of vacuum grease. (Photo No 2).

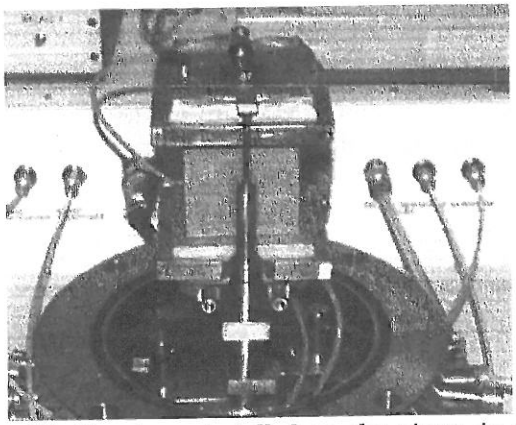

Fig. 21. Specimen installed on the piston in the conventional triaxial apparatus. The specimen is left to defrost under a partial vacuum of approximately 20 kPa. (Photo No 4).

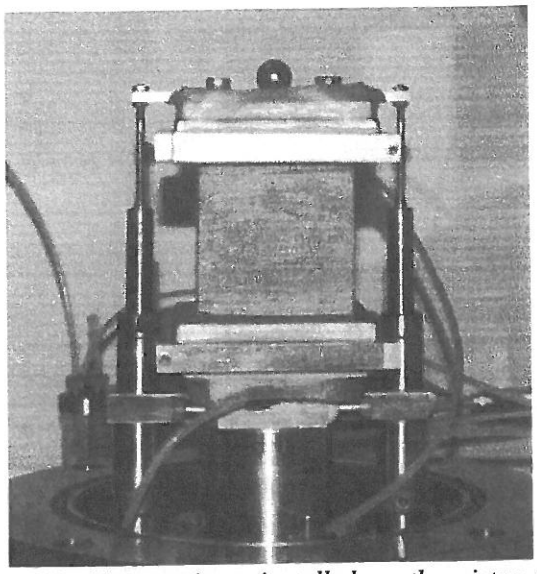

Fig. 22. The specimen installed on the piston in the conventional triaxial apparatus. The two displacement transducers are mounted on the top platen and on the piston itself. (Photo No 5).

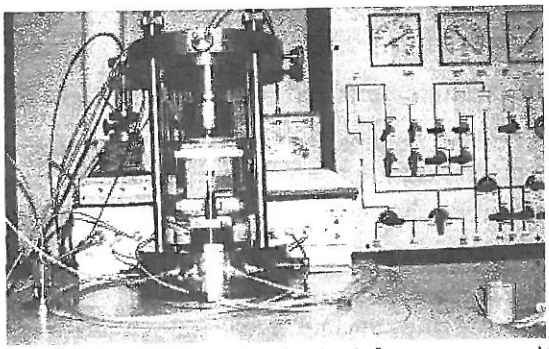

Fig. 23. The conventional triaxial apparatus with a cubical specimen placed inside the chamber. The volume change is measured by the scale located just behind the chamber. (Photo No 6).

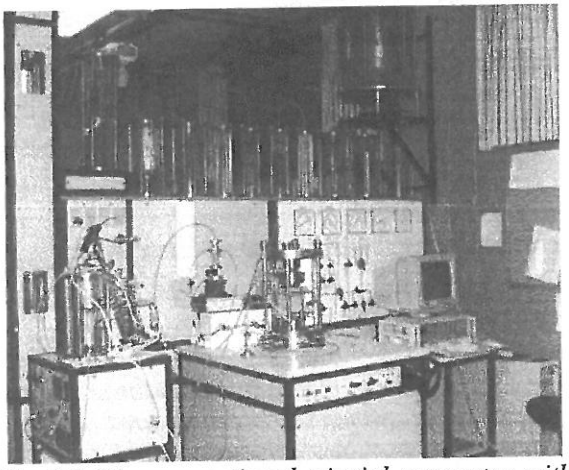

Fig. 24. The conventional triaxial apparatus with accessories such as the back pressure system (shown in the lower left corner), data collection and control devices (shown in the lower right corner) and saturation system (located in the back). (Photo No 7).

4.2.2 True triaxial apparatus

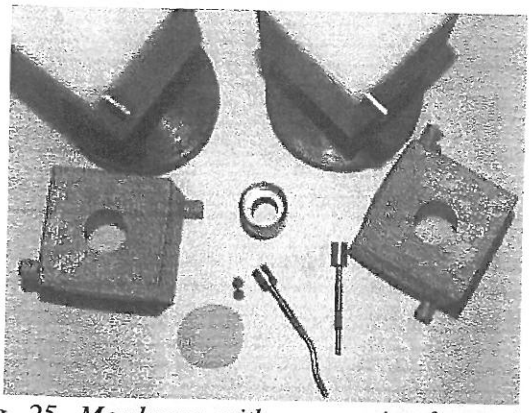

Fig. 25. Membrane with accessories for testing frozen cubical specimens in the true triaxial apparatus. The two objects placed on top (in the figure) are used in the production of the membranes. The metal ring (shown in the middle) is used to create the circular holes in the membranes. The filter stones are placed in the tip of the metal gadgets prior to their attachment to a membrane. (Photo No 21).

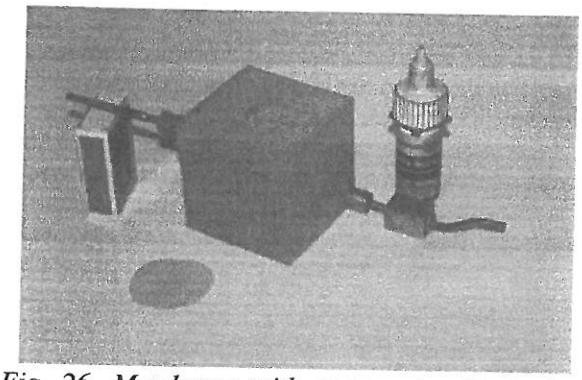

Fig. 26. Membrane with accessories for testing frozen cubical specimens in the true triaxial apparatus. The two gadgets sticking out of the membrane work as part of the drainage system. During a test, the lowermost gadget is connected to the scale, whereas the uppermost gadget is connected to the absolute pressure transducer. The super glue is together with the rubber disc used to close the membrane. (Photo No 35).

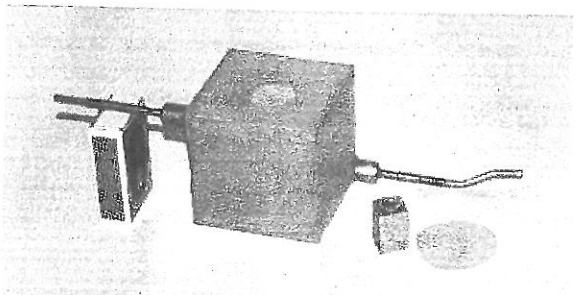

Fig. 27. Membrane with accessories for testing frozen cubical specimens in the true triaxial apparatus. (Photo No 36).

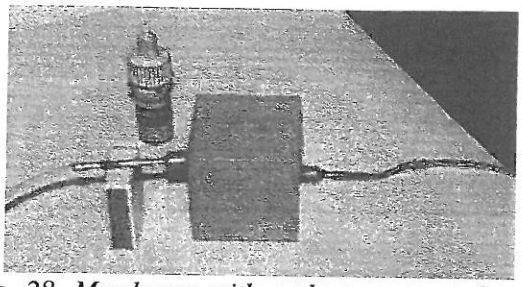

Fig. 28. Membrane with gadgets connected to a vacuum pump through soft rubber tubes. (Photo No 40).

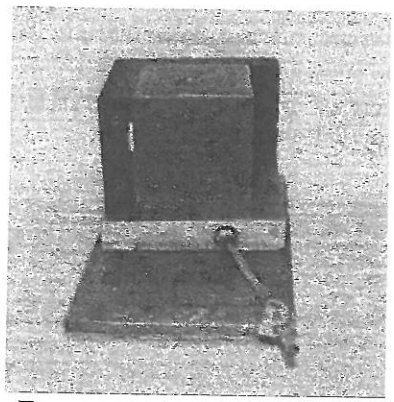

Fig. 29. Frozen specimen in partly dismounted spilt mould placed in a freezer. The remaining platens are removed prior to manoeuvring the specimen into the membrane. (Photo No 39).

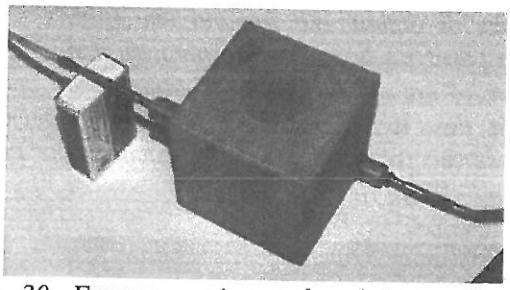

Fig. 30. Frozen specimen placed in membrane. The rubber disc has now been glued onto the membrane using the super glue mentioned previously. A partial vacuum of app. 20 kPA is applied to the specimen at this point. (Photo No 41).

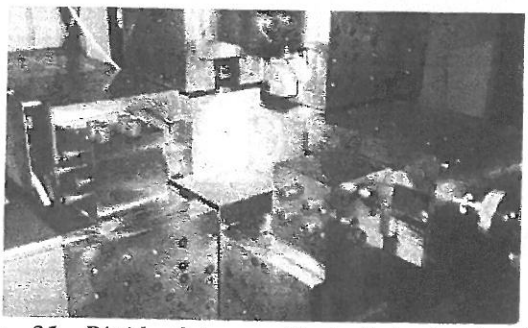

Fig. 31. Rigid platens with built-in load cells mounted in the true triaxial apparatus. The platens have been coated with a thin layer of vacuum grease. (Photo No 37).

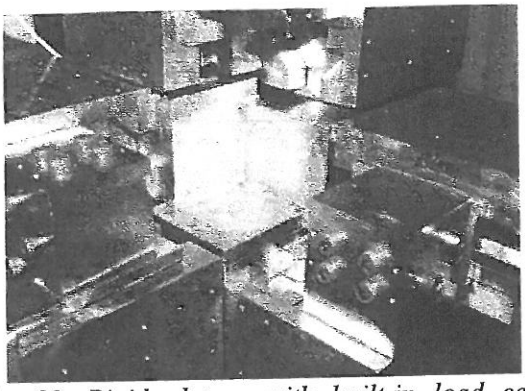

Fig. 32. Rigid platens with built-in load cells mounted in the true triaxial apparatus. The platens have now been lubricated with two thin layers of vacuum grease and a rubber sheet to minimise shear forces. (Photo No 38).

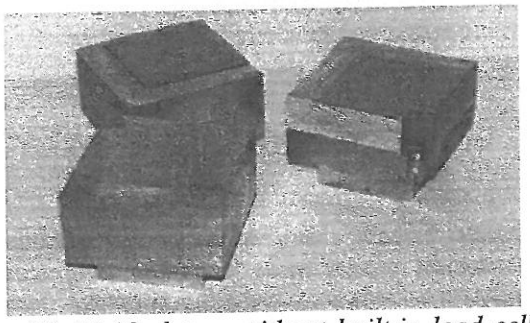

Fig. 33. Rigid platens without built-in load cells. Two platens have been lubricated with two thin layers of vacuum grease and one rubber sheet. One plate has been coated only with a single thin layer of grease This plate is going to be placed right next to the side of the cubical specimen where the rubber disc was glued onto the membrane. (Photo No 45).

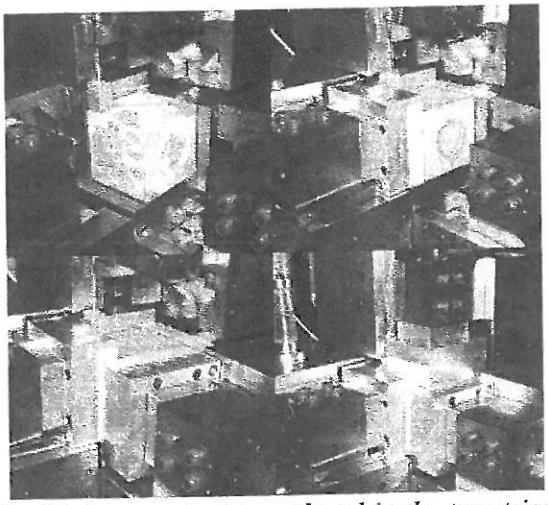

Fig. 34. Frozen specimen placed in the true triaxial apparatus and the process for mounting remaining platens. The specimen is left to defrost under a partial vacuum of approximately 20 kPa for at least six hours before the last three platens are mounted. (Photos No 42, 46, 47 & 48).

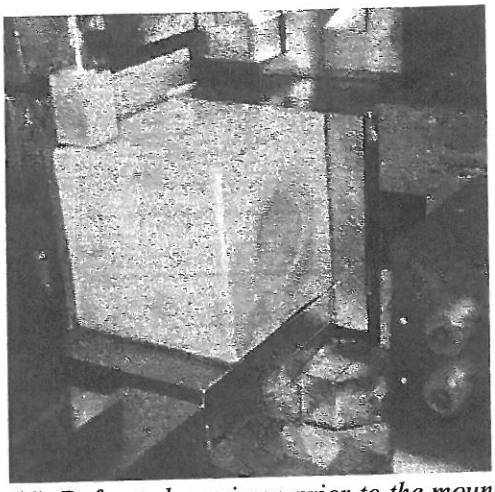

Fig. 35. Defrosted specimen prior to the mounting of the remaining three platens. Contact glue has been used around the rubber disc to strengthen the joint. The metal gadget placed on top of the specimen fits exactly into the cut in the top plate, see figure 33. (Photo No 43).

4.3 Diverse

This subsection includes some photos that have been taken to illustrate certain issues.

4.3.1 Blocks

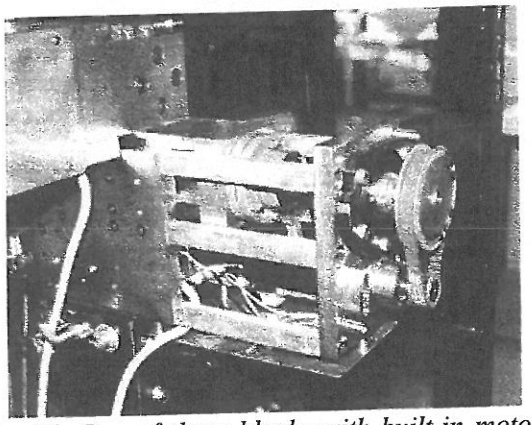

Fig. 36. One of three blocks with built-in motors and screw spindles. (Photo No 8).

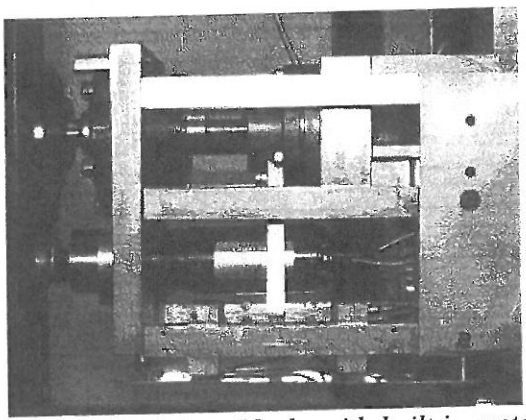

Fig. 37. One of three blocks with built-in motors and screw spindles. (Photo No 9).

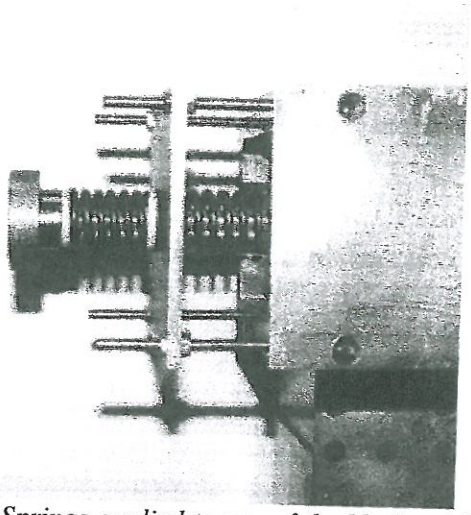

Fig. 38. Springs applied to one of the blocks without built-in motors. A spring was placed at each side of the plate to hinder the development of gaps between rigid platens during a test. The springs affected the test results in an undesirable manner and they were therefore removed afterwards. (Photo No 13).

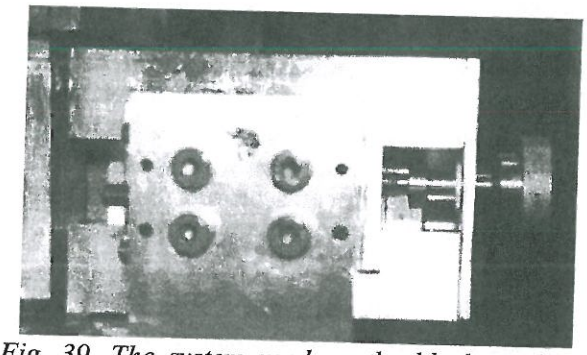

Fig. 39. The system used on the blocks without built-in motors. The system produced more consistent test results than the system with the built-in springs. (Photo No 14).

4.3.2 Types of rigid platens

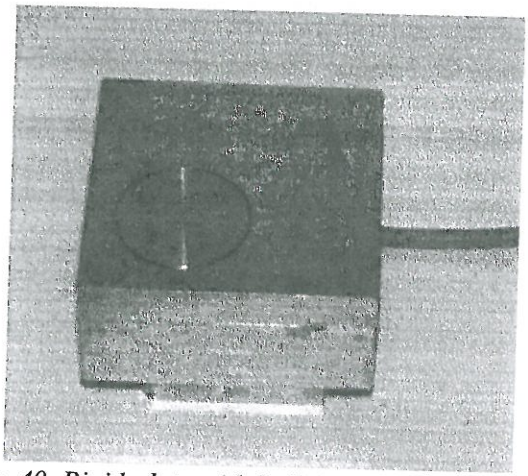

Fig. 40. Rigid plate with built-in load cell for testing 70x70x70mm specimens. (Photo No 15).

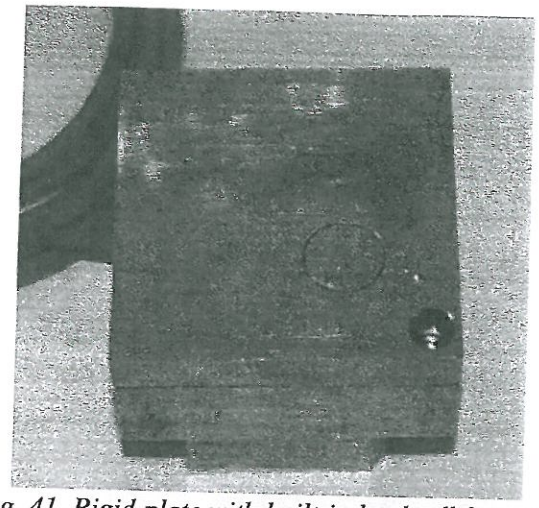

Fig. 41. Rigid plate with built-in load cell for testing 50x50x50mm specimens. (Photo No 16).

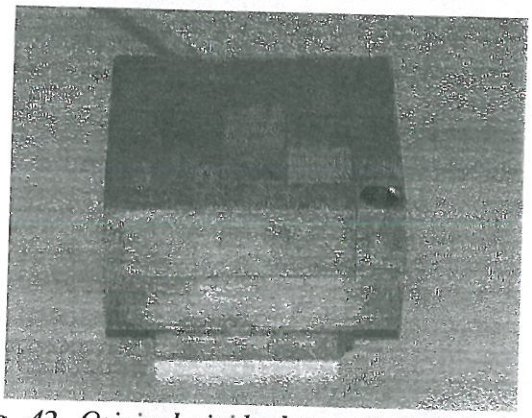

Fig. 42. Original rigid plate with built-in load cells and shear stress transducers for testing 70x70x70mm specimens. (Photo No 17).

4.3.3 The true triaxial apparatus

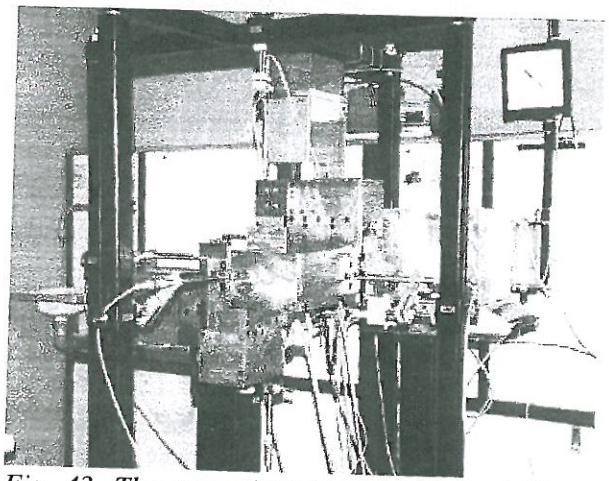

Fig. 43. The true triaxial apparatus at Aalborg University. The scale (located to the far right) is used to measure volume changes. The transducers mounted on the reference system (black bars around the apparatus) are used to measure displacements. Part of the water saturation system is shown in the upper right corner. (Photo No 49).

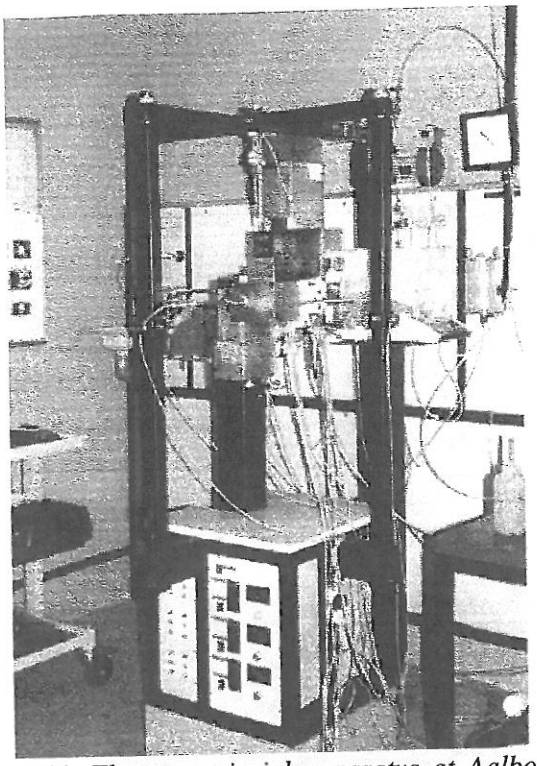

Fig. 44. The true triaxial apparatus at Aalborg University. The box shown in the bottom contains some electronical equipment. (Photo No 50).

4.3.4 Post test photos

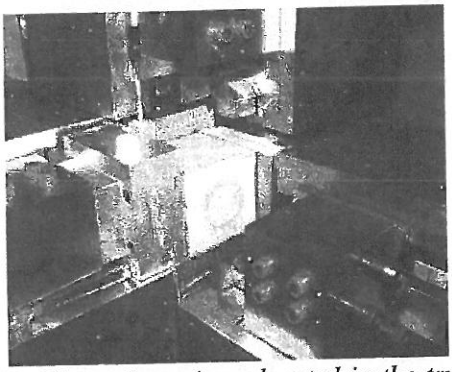

Fig. 45. Sheared specimen located in the true triaxial apparatus with two platens removed. Shear bands were not detected. (Photo No 51).

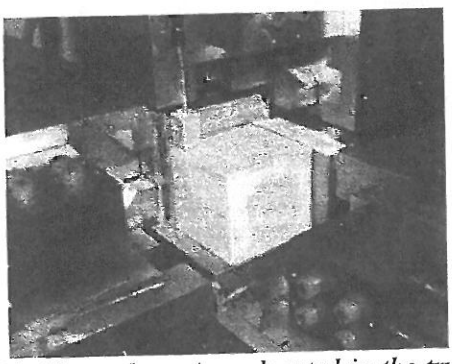

Fig. 46. Sheared specimen located in the true triaxial apparatus with three platens removed. Shear bands were not detected. (Photo No 52).

5 REFERENCES

Arthur, J.R.F. (1988). *Cubical Devices: Versatility and Constraints. Advanced Triaxial Testing of Soil and Rock.* ASTM STP 977, 743-765.

Borup, M. & Hedegaard, J. (1995). *Data Report 9403 - Barskap Sand No 15.* AAU Geotechnical Engineering Papers. Aalborg University.

Gudehus, G. (1971). *Discussion.* Proceedings of the Roscoe Memorial Symposium, G. T. Foulis, Henley on Thames, 373-375.

Hambly, E. C. (1967). *A New Triaxial Apparatus.* Geotechnique. Vol 19, No. 2, 1969, 307-309.

Ibsen, L.B. & Brødker, L. (1994). *Data Report 9301 - Barskap Sand No 15.* AAU Geotechnical Engineering Papers. Aalborg University.

Ibsen, L.B & Praastrup, U. . (2000). *The Danish Rigid Boundary True Triaxial Apparatus for Soil Testing.* Submitted to Geotechnical Testing Journal.

Jakobsen, K.P. & Praastrup, U. 1998. *"Drained Triaxial Tests on Eastern Scheldt Sand"*, AAU Geotechnical Engineering Papers. Aalborg University.

Jakobsen, K.P. (1998). *"Undrained Triaxial Tests on Eastern Scheldt Sand"*, AAU Geotechnical Engineering Papers. Aalborg University.

Pearce, J. A. (1972). *A New Triaxial Apparatus.* Proceedings of the Roscoe Memorial Symposium, G. T. Foulis, Henley on Thames, 330-339.

Praastrup, U. (1999a). *Manual for Udførelse af Triaxialforsøg ved AAU - Kap. 2. Standardkonfiguration.* AAU Geotechnical Engineering Papers. Aalborg University.

Praastrup, U. (1999b). *Manual for Udførelse af Triaxial Forsøg ved AAU - Kap. 3. Programbeskrivelse.* AAU Geotechnical Engineering Papers. Aalborg University.

Praastrup, U. (2000). *Manual for Udførelse af Triaxialforsøg ved AAU - Appendix 1. Programmer til Triaxial Forsøg.* AAU Geotechnical Engineering Papers. Aalborg University.

Praastrup, U. Jakobsen, K.P. & Ibsen, L.B. (1999) *"Two Theoretical Consistent Methods for Analysing Triaxial Tests"*, Computers & Geotechnics, 25, 157-170.